On the upstream mobility scheme for two-phase flow in porous media

Siddhartha Mishra, Jérôme Jaffré

INSTITUT NATIONAL DE RECHERCHE EN INFORMATIQUE ET EN AUTOMATIQUE

On the upstream mobility scheme for two-phase flow in porous media

Siddhartha Mishra — Jérôme Jaffré

N° 6789

Décembre 2008

Thème NUM

Rapport de recherche

ISSN 0249-6399 ISRN INRIA/RR--6789--FR+ENG

INSTITUT NATIONAL
DE RECHERCHE
EN INFORMATIQUE
ET EN AUTOMATIQUE

INRIA

centre de recherche
PARIS - ROCQUENCOURT

On the upstream mobility scheme for two-phase flow in porous media

Siddhartha Mishra * , Jérôme Jaffré †

Thème NUM — Systèmes numériques
Équipes-Projets Estime

Rapport de recherche n° 6789 — Décembre 2008 — 33 pages

Abstract: When neglecting capillarity, two-phase incompressible flow in porous media is modelled as a scalar nonlinear hyperbolic conservation law. A change in the rock type results in a change of the flux function. Discretizing in one-dimensional with a finite volume method, we investigate two numerical fluxes, an extension of the Godunov flux and the upstream mobility flux, the latter being widely used in hydrogeology and petroleum engineering. Then, in the case of a changing rock type, one can give examples when the upstream mobility flux does not give the right answer.

Key-words: Two-phase flow in porous media, upstream mobilities, hyperbolic conservation laws, entropy condition, finite difference method, finite volume method.

* Center of Mathematics for Applications, University of Oslo, Oslo-0316, Norway (siddharm@cma.uio.no)
† INRIA, BP 105, 78153 Le Chesnay Cedex, France (Jerome.Jaffre@inria.fr)

Centre de recherche INRIA Paris – Rocquencourt
Domaine de Voluceau, Rocquencourt, BP 105, 78153 Le Chesnay Cedex
Téléphone : +33 1 39 63 55 11 — Télécopie : +33 1 39 63 53 30

Sur le schéma aux mobilités amont pour les écoulements diphasiques en milieu poreux

Résumé : En négligeant la capillarité, un écoulement diphasique incompressible est modélisé par une loi de conservation scalaire hyperbolique non-linéaire. Un changement dans le type de roche entraîne un changement de la fonction flux. En discrétisant en dimension un avec une méthode de volumes finis nous étudions deux flux numériques, une extension du flux de Godunov et le flux des mobiltés amont, ce dernier étant largement utilisé en hydrologie et en ingéniérie pétrolière. Dans le cas d'un changement de type de roche on peut alors donner des exemples où le flux des mobiltés amont ne donne pas une solution correcte.

Mots-clés : Ecoulement diphasique en milieu poreux, mobilités amont, lois de conservation hyperboliques, condition d'entropie, méthode de différences finies, méthode de volumes finis.

1 Introduction

Under the assumptions that capillary effects are neglected, two-phase flow in a porous medium is modeled by a nonlinear hyperbolic equation. In many applications, the porous medium is not homogenous. The flow domain has to be divided into several subdomains corresponding to different types of rock separated by lines or surfaces along which, not only the porosity and the absolute permeability of the rock type change but the relative permeabilities also differ. This situation is modeled by a single conservation law with a flux function discontinuous in the space variable. Numerical methods designed to simulate the flow have to be devised to take into account the discontinuities in the flux function.

In this paper, we compare different numerical schemes of the finite difference or finite volume type that are used to simulate two-phase flow in porous media with changing rock types. We restrict ourselves to the one dimensional case. In the multidimensional case, most numerical methods still use the one dimensional flux calculation in the direction normal to the boundaries of the discretization cells. We also focus on the numerical flux calculation.

Conservation laws with discontinuous coefficients arise in several other situations in Physics and Engineering like in modeling continuous sedimentation in clarifier thickener units used in waste water treatment plants (See [12], [13], [8]), in traffic flow on highways with changing surface conditions (see [23]) and in ion etching used in the semiconductor industry (see [24]). A detailed account of the above applications can be found in [26]. Consequently, equations of this type have been studied extensively from both a theoritical as well as a numerical point of view.

In particular, for equations governing two-phase flow in porous media, the numerical scheme that is commonly used by the petroleum engineers is the upstream mobility flux scheme (see [7, 25, 9, 20]). An alternative finite difference (volume) method of the Godunov type based on exact solutions of the Riemann problem was presented in Adimurthi, Jaffre and Gowda ([2]). The above paper also addressed the problem of prescribing correct entropy conditions at the interface between rock types and showing the uniqueness of the entropy solution. The solutions computed by the Godunov type scheme was shown to converge to the entropy solution. The numerical flux developed in [2] is similar to that used by Kaasschieter in [21] although written in a more compact form.

It is natural to ask whether the solution computed by the upstream mobility flux scheme also converges to the entropy solution and compare its numerical performance with other schemes like the one in [2] and that of Towers ([29], [30]). The goal of this paper is to address these questions.

In this paper, we will give an explicit representation of the upstream mobility flux scheme for a medium consisting of two rock types and show that the numerical flux is monotone. This will help us to obtain estimates in L^∞. We will then use a suitable modification of the singular mapping technique to show that the approximate solution converges to a weak solution of the continuous problem. . The key point of this paper is to address whether this weak solution is a entropy solution or not. We show by various numerical experiments that the solutions computed by the upstream mobility flux scheme are not consistent with the interface entropy condition of [2]. Furthermore, we construct numerical experiments for the case where only the absolute permeability changes. In this

case, the solutions given by the scheme do not converge to the entropy solution pointwise and differ qualitatively from the entropy solution. The lack of entropy consistency leads us to suggest that the upstream mobility flux scheme may not be the correct numerical method to simulate two-phase flow in porous media with changing rock types and should be replaced by the Godunov type scheme develop in [2].

This paper is organised as follows, In section 2, we describe the equations governing two phase flow in porous media with heterogenities. In section 3, we summarise the mathematical theory for single conservation laws with discontinuous flux developed in [1], [2] and mention the well posedness results. Section 4 is devoted to describing finite difference schemes of the Godunov type as well as the upstream mobility flux scheme. The convergence analysis for the upstream mobility flux scheme is carried out in section 5. We give explicit representation formula for the flux, show that it is monotone and use a variation of the singular mapping technique to show convergence to a weak solution. The core of this paper is in section 6 where we address the question of entropy consistency. First, we consider numerical experiments for the case where only the absolute permeability changes and discuss the entropy behaviour of the solutions. Next, we construct examples of the case where the relative permeability also changes and show that the scheme is not consistent with the interface entropy condition of [2]. We derive some conclusions from this paper in section 7.

2 Two-phase flow equations

Capillary-free two-phase incompressible flow is modeled by the following scalar nonlinear hyperbolic equation

$$\phi \frac{\partial S}{\partial t} + \frac{\partial f}{\partial x} = 0$$

where ϕ is the porosity of the rock, $S = S_1$ is the saturation of phase 1 which lies in a bounded interval $[0, 1]$. The flux function f is the Darcy velocity φ_1 of phase 1 and has the form

$$f = \varphi_1 = \frac{\lambda_1}{\lambda_1 + \lambda_2}[q + (g_1 - g_2)\lambda_2].$$

Here $q = \varphi_1 + \varphi_2$ denotes the total Darcy velocity where $\varphi_\ell, \ell = 1, 2$, denotes the Darcy velocity of phase ℓ with, for the second phase,

$$\varphi_2 = \frac{\lambda_2}{\lambda_1 + \lambda_2}[q + (g_2 - g_1)\lambda_1].$$

Since the flow is assumed to be incompressible, the total Darcy velocity q is independent of the space variable x.

The quantities λ_ℓ, $\ell = 1, 2$ may be called effective mobilities. These are products of the absolute permeability K by the mobilities k_ℓ :

$$\lambda_\ell = K k_\ell, \ \ell = 1, 2.$$

The absolute permeability K may depend on x and the quantities k_ℓ and λ_ℓ are functions of S which satisfy the following properties :

$$\begin{array}{l} k_1 \text{ and } \lambda_1 \text{ are increasing functions of } S, \ k_1(0) = \lambda_1(0) = 0, \\ k_2 \text{ and } \lambda_2 \text{ are decreasing functions of } S, \ k_2(1) = \lambda_2(1) = 0. \end{array}$$

We also shall assume that these functions are smooth functions of the saturation S and so is the flux function f.

The gravity constants g_ℓ, $\ell = 1, 2$ of the phases are

$$g_\ell = g\rho_\ell \frac{dx}{dz},\ \ell = 1, 2\,,$$

with g the acceleration due to gravity, ρ_ℓ the density of phase ℓ and z is the vertical position of the point of abscissa x.

Observe that with the above hypothesis, f is a smooth (say Lipschitz) function with at most one local maxi with $f(0) = 0$ and $f(1) = q$ respectively.

In many practical situations, the porous medium is heterogenous. For example the medium may consist of two rock types separated at the interface ($x = 0$). In this case, the porosity, the absolute permeability and the relative permeability change across the interface and the flow is modeled by the following equations:

$$\begin{array}{l}(H(x)\phi^+ + (1 - H(x))\phi^-)S_t + (H(x)f^+(S) + (1 - H(x))f^-(S))_x = 0,\\ S(0, x) = S_0(x)\end{array} \tag{2.1}$$

where H is the Heaviside function and the indices - and + refer to to the left and the right of the interface respectively. The flux functions are given by the following,

$$f^\pm = \frac{\lambda_1^\pm}{\lambda_1^\pm + \lambda_2^\pm}[q + (g_2 - g_1)\lambda_2^\pm], \quad \lambda_i^\pm = K^\pm k_i^\pm. \tag{2.2}$$

See Figure 2.1 for notations and the shapes of the flux functions when $q < 0, g_2 > g_1$. Note that the flux functions may also intersect as we will see in the numerical experiments of Section 6.

Rock type I	**Rock type II**
$\phi^-,\ K^-,\ k_1^-,\ k_2^-$	$\phi^+,\ K^+,\ k_1^+,\ k_2^+$
$0 \le S \le 1$	$0 \le S \le 1$
$f \equiv f^-$	$f \equiv f^+$

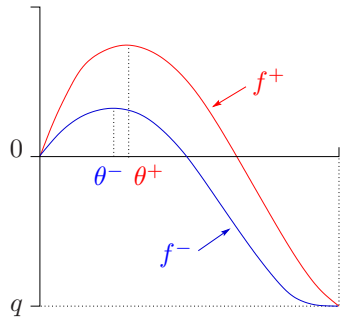

Figure 2.1: Constants, mobilities and fluxes for two rock types

Equations (2.1) with flux functions (2.2) are a special case for the more general single conservation law with flux function discontinuous in the space variable considered in [2]. Flux functions f^- and f^+ satisfy the following hypothesis,

H$_1$.f^-, f^+ are smooth (say Lipschitz) on $[0, 1]$.
H$_2$.$f^-(0) = f^+(0) = 0$, $f^-(1) = f^+(1) = q$.
H$_3$.f^-, f^+ have exactly one local maximum in $[0, 1]$ with $\theta^- =$ argmax (f^-)

and $\theta^+ = \text{ argmax } (f^+)$.

Note that these are precisely the hypotheses for the fluxes assumed in [2].

3 The continuous problem

As presented in the previous section, a change of rock types leads to a single conservation law with a flux function discontinuous in the space variable. An entropy theory has been developed for equations of the form (2.1) with the fluxes satisfying the hypothesis H_1, H_2, H_3. We summarize some of the results for the benefit of the reader.

Even in the case where the flux is continuous, it is well known that solutions of equations of the above type develop discontinuities in finite time even for smooth initial data. Hence as in the continuous case, weak solutions S of (2.1) are sought and defined as satisfying

$$\int_{\mathbb{R}}\int_{\mathbb{R}_+} S\varphi_t dxdt + \int_{\mathbb{R}}\int_{\mathbb{R}_+} (H(x)f^+(S) + (1-H(x)f^-(S))\varphi_x dxdt + \int_{\mathbb{R}} S_0(x)\phi(0,x)dx = 0, \quad \forall \varphi \in C_0^\infty(\overline{\mathbb{R}\times\mathbb{R}_+}). \quad (3.1)$$

It is easy to check that S is a weak solution of (2.1) iff it satisfies in the weak sense,

$$\begin{array}{lcll} S_t + (f^-(S))_x & = & 0, & x<0, \quad t>0, \\ S_t + (f^+(S))_x & = & 0, & x>0, \quad t>0, \\ S(0,x) & = & S_0(x), & \forall\, x\in\mathbb{R}, \end{array}$$

and the following interface Rankine Hugoniot condition,

$$f^+(S^+(t)) = f^-(S^-(t)) \qquad \text{for almost all } t,$$

where

$$S^+(t) = \lim_{x\to 0+} S(x,t), \qquad\qquad S^-(t) = \lim_{x\to 0-} S(x,t).$$

It is well known that weak solutions for a single conservation law are not necessarily unique. Additional admissibility criteria termed as entropy conditions need to be imposed for uniqueness. For equations of the form (2.1), it is natural to impose the standard Kruzkhov entropy conditions away from the interface $x = 0$. These can be stated in terms of the entropy flux pairs which are defined as

Entropy pairs: $\{\varphi_i, \psi_i\}_{i=1,2}$ is said to be an entropy pair for (2.1) if φ_i is convex in $[0,1]$ and $\psi_1'(\theta) = \phi_1'(\theta)f^{+\prime}(\theta), \psi_2'(\theta) = \phi_2'(\theta)f^{-\prime}(\theta)$ for $\theta \in [0,1]$.

Let $S_0 \in L^\infty(\mathbb{R})$ be the initial data with $0 \le S_0(x) \le 1, \forall x \in \mathbb{R}$, and let S be a weak solution of (3.1) with $0 \le S(x,t) \le 1, \forall (x,t) \in \mathbb{R}\times\mathbb{R}_+$.

Interior entropy condition: With S_0 and S as above, S is said to satisfy an interior entropy condition if for any entropy pairs $(\varphi_i,\psi_i)_{i=1,2}, S$ satisfies in the sense of distributions

$$\begin{array}{lcll} \dfrac{\partial \varphi_1(S)}{\partial t} & + & \dfrac{\partial \psi_1(S)}{\partial x} \le 0, & \forall x>0, t>0. \\ \dfrac{\partial \varphi_2(S)}{\partial t} & + & \dfrac{\partial \psi_2(S)}{\partial x} \le 0, & \forall x<0, t>0 \end{array} \quad (3.2)$$

But for equation (2.1), interior entropy conditions like the one above are not sufficient to guarantee uniqueness and we need to impose an additional entropy condition at the interface. The central issue in the analysis of conservation laws with discontinuous flux is the choice of this interface entropy condition. In [2], the following interface entropy condition was used.

Interface entropy condition: With S_0 and S as above, assume that $S^+(t) = \lim_{x\to 0^+} S(x,t)$ and $S^-(t) = \lim_{x\to 0^-} S(x,t)$ exist for almost all $t > 0$ and define,

$$\begin{aligned} L &= \{t > 0;\ S^-(t) \in (\theta^-, 1], S^+(t) \in [0, \theta^+)\}\,, \\ U &= \{t \in L;\ S^+(t) = S^-(t) = 1\} \cup \{t \in L;\ S^-(t) = S^+(t) = 0\}\,. \end{aligned}$$

Then S is said to satisfy the interface entropy condition if

$$\text{meas } \{L \setminus U\} = 0\,. \tag{3.3}$$

This means that the characteristics must connect back to the x-axis on at least one side of the jump in the flux i.e., undercompressive waves are not allowed. Undercompressive waves i.e., $(f^{+\prime}(S^+) > 0, \quad f^{-\prime}(S^-) < 0)$ are unrealistic physically as information is not taken from the initial line.

S is defined to be an entropy solution of (2.1) if it is a weak solution and it satisfies both the interior as well as the interface entropy condition. With this concept of entropy solution, the following wellposedness result was obtained in [2], under the following hypotheses on the initial data:

IN$_1$. S_0 is such that $0 \le S_0(x) \le 1, \quad \forall \quad x \in \mathbb{R}$,
IN$_2$. $N(f^-, f^+, S_0) \le C < +\infty$,

where $N(f^-, f^+, S_0)$ is an estimator of the total variation of the flux function evaluated at S_0. This estimator will be defined precisely below in Section 4.

We also need the following definition,

Regular solution. S is said to be a regular solution of (2.1) if the discontinuities of S form a discrete set of Lipschitz curves.

The well posedness result is given by

THEOREM 3.1 *Let S_0 satisfy hypotheses IN_1, IN_2 and f^-, f^+ satisfy hypotheses H_1, H_2, H_3. Then there exists a weak solution $S \in L^\infty(\mathbb{R} \times \mathbb{R}+)$ of (2.1) satisfying the following,*
(1) For almost all $t > 0$ and $x \in \mathbb{R}$, $\quad S(x_-, t), S(x_+, t)$ exist.
(2) S satisfies the interior entropy condition (3.2).
(3) If S is a regular solution, then S satisfies the interface entropy condition (3.3) and it is unique.

Uniqueness is proved by using a Kruzkhov type doubling of variables argument. For details, see [2]. Existence was shown by showing that a Godunov type finite difference scheme converges to a weak solution and is consistent with the entropy conditions.

We would also like to mention that more recently hypotheses on the fluxes have been relaxed considerably to include fluxes of the concave-convex type as in [27, 4] , and with finitely many extrema as in [5]. Similarly schemes of the Enquist-Osher (EO) type have been considered in [1, 27]. It is to be observed

that equations of the type (2.1) are special cases of the more general single conservation law with discontinuous coefficient of the form,

$$u_t + (f(k(x), u))_x = 0, \qquad u(0, x) = u_0(x)$$

The wellposedness and numerical methods for this problem are addressed in a forthcoming paper [6]. We must also mention that an entropy theory for equations of the above type (including a degenerate parabolic term) has been developed by Karlsen, Risebro and Towers in [18]. In [29, 30], the author developed staggered mesh algorithms of the Godunov and Enquist Osher type for the multiplicative case i.e. $f(k, u) = k(x)f(u)$. The case with a degenerate parabolic term was handled in [18] and the time dependent case in [10]. The entropy condition of [19] agrees with that of [2] in many cases but differs in certain cases. See Section 6 for a discussion of different entropy conditions for equation (2.1). For the rest of this paper, we will use the entropy framework developed in [2].

4 Finite Difference Schemes

In this section, we present finite difference schemes using for numerical flux either the extended Godunov flux [2] or the upstream mobility flux used in the petroleum industry for the simulation of two-phase flow in porous media.

Let f be a Lipschitz continuous function. Then the Godunov flux corresponding to f is given by

$$F_g(a, b) = \begin{cases} \min\limits_{\theta\in[a,b]} f(\theta) & \text{if} \quad a < b, \\ \max\limits_{\theta\in[b,a]} f(\theta) & \text{if} \quad a \geq b, \end{cases} \tag{4.1}$$

The subscript g stands here for Godunov in order to differentiate this flux from the upstream mobility flux that we will introduce later. This flux was first proposed in [17] and is very popular in the numerical analysis of conservation laws. It is based on exact solutions of the Riemann problem. Let F_g^- and F_g^+ be the Godunov fluxes corresponding to the fluxes f^- and f^+ respectively.

In the case of two-phase flow, the flux functions f^-, f^+ satisfy hypotheses $\mathrm{H}_1, \mathrm{H}_2, \mathrm{H}_3$ and the formula (4.1) can be simplified as follows,

$$\begin{aligned} F_g^-(a, b) &= \min\{f^-(\min(a, \theta_-), f^-(\max(\theta_-, b)\}, \\ F_g^+(a, b) &= \min\{f^+(\min(a, \theta_+), f^+(\max(\theta_+, b)\}. \end{aligned}$$

These formulas were introduced in [2] and are simpler to implement than the general formula (4.1).

Also, following [2], they extend easily to define the interface Godunov flux $\overline{F}_g$ based on the exact solution of the Riemann problem for (2.1):

$$\overline{F}_g(a, b) = \min\{f^-(\min(a, \theta_-), f^+(\max(\theta_+, b)\} \tag{4.2}$$

We remark that the above interface flux coincides with the interface flux obtained in [21] for which expression (4.2) represents a compact form, very easy to use for computational purposes. It is also easy to check that the interface

flux $\overline{F}_g$ is Lipschitz is both variables, nondecreasing in the first variable and nonincreasing in the second variable. Note that the interface flux satisfies

$$\overline{F}_g(0,0) = f^-(0,0) = f^+(0,0) = 0, \quad \overline{F}_g(1,1) = f^-(1,1) = f^+(1,1) = q,$$

but is not consistent.

Equipped with the definition of the numerical fluxes, we proceed to describe the mesh. Let $h > 0$ and define the space grid points as follows:

$$x_{-1/2} = x_{1/2} = 0, \quad x_{j+1/2} = j\ h \quad \text{for } j \geq 0, \quad x_{j-1/2} = jh \quad \text{for } j \leq 0.$$

We will also use the midpoints of the intervals:

$$x_j = \left(\frac{2j-1}{2}\right) h \quad \text{for } j \geq 1, \quad x_j = \left(\frac{2j+1}{2}\right) h \quad \text{for } j \leq -1.$$

For time discretization the time step is $\Delta t > 0$, and let $t_n = n\Delta t,\ \lambda = \frac{\Delta t}{h}$.

For an initial data $S_0 \in L^\infty(\mathbb{R})$ we define

$$S^0_{j+1} = \frac{1}{h}\int_{x_{j+1/2}}^{x_{j+3/2}} S_0(x)dx \quad \text{if} \quad j \geq 0, \quad S^0_{j-1} = \frac{1}{h}\int_{x_{j-3/2}}^{x_{j-1/2}} S_0(x)dx \quad \text{if} \quad j \leq 0.$$

Now we can define the Godunov type finite difference scheme $\{S^n_j\}$ inductively as follows:

$$\begin{array}{rcll} S^{n+1}_1 &=& S^n_1 - \lambda(F^+_g(S^n_1, S^n_2) - \overline{F}_g(S^n_{-1}, S^n_1)), & \\ S^{n+1}_j &=& S^n_j - \lambda(F^+_g(S^n_j, S^n_{j+1}) - F^+_g(S^n_{j-1}, S^n_j)) & \text{if } j > 1, \\ S^{n+1}_{-1} &=& S^n_{-1} - \lambda(\overline{F}_g(S^n_{-1}, S^n_1) - F^-_g(S^n_{-2}, S^n_{-1})), & \\ S^{n+1}_j &=& S^n_j - \lambda(F^-_g(S^n_j, S^n_{j+1}) - F^-_g(S^n_{j-1}, S^n_j)) & \text{if} \quad j < -1. \end{array} \tag{4.3}$$

Observe that this is the standard Godunov scheme for $j \neq \pm 1$, that is, away from $x = 0$,

For $S_0 \in L^\infty(\mathbb{R})$ and grid length h and Δt with $\lambda = \frac{\Delta t}{h}$ fixed, define the piecewise constant function $S_h \in L^\infty(\mathbb{R} \times \mathbb{R}_+)$ associated with $\{S^n_j\}$ calculated by the scheme (4.3):

$$S_h(x,t) = S^n_j \quad \text{for } (x,t) \in [x_{j-1/2}, x_{j+1/2}) \times [n\Delta t,\ (n+1)\Delta t), \quad j \neq 0. \tag{4.4}$$

The above Godunov type scheme was analysed in [2]. For this analysis we need to introduce

$$\begin{aligned} N^g_h(f^-, f^+, S_0) \quad = \quad & \sum_{j<-1} |F^-_g(S^0_j, S^0_{j+1}) - F^-_g(S^0_{j-1}, S^0_j)| \\ & + \sum_{j>1} |F^+_g(S^0_j, S^0_{j+1}) - F^+_g(S^0_{j-1}, S^0_j)| \\ & + |\overline{F}_g(S^0_{-1}, S^0_1) - F^-_g(S^0_{-2}, S^0_{-1})| \\ & + |F^+_g(S^0_1, S^0_2) - \overline{F}_g(S^0_{-1}, S^0_1)|, \end{aligned}$$

$$N_g(f^-, f^+, S_0) = \sup_{h>0} N^g_h(f^-, f^+, S_0).$$

It is easy to see that if $S_0 \in BV(\mathbb{R})$, then $N_g(f^-, f^+, S_0) \leq C||S_0||_{BV}$, where C is a constant depending only on the Lipschitz constants of f^- and f^+.

The following convergence theorem was proved, Let $M = \max Lip\{f^-, f^+\}$,

THEOREM 4.1 *Assume that λ, M satisfies the CFL condition $\lambda M \leq 1$. Let $S_0 \in L^\infty(\mathbb{R})$ such that $0 \leq S_0(x) \leq 1$ for all $x \in \mathbb{R}$ and $N_g(f^-, f^+, S_0) < \infty$. For $h > 0$, let $\lambda = \frac{\Delta t}{h}$ and S_h be the corresponding calculated solution given by (4.3), (4.4). Then there exists a subsequence $h_k \to 0$ such that S_{h_k} converges almost everywhere to a weak solution S of (2.1) satisfying the interior entropy condition. Suppose the discontinuities of every limit function S of $\{S_h\}$ form a discrete set of Lipschitz curves, then $S_h \to S$ in $L^\infty_{loc}(\mathbb{R}_+, L^1_{loc}(\mathbb{R}))$ as $h \to 0$, and S satisfies the interface entropy condition.*

The convergence of the scheme was proved by using the singular mapping technique which we will also use in section 5 albeit with modifications. The limit solution obtained was shown to be consistent with the interior as well as the interface entropy condition. The key point in the proof of consistency with the interface entropy condition was the use of a contradiction argument using s test function. The reader is referred to [2] for details. We will use similar ideas in the next section. Some numerical experiments involving this Godunov type scheme are shown in section 6.

As mentioned earlier, staggered mesh schemes were proposed in [29], [30] and [18] for general single conservation laws with discontinuous flux. In the simplified case of a single discontinuity in the flux, the staggered mesh scheme of the Godunov type can also be written in the form (4.3) by replacing the interface Godunov flux $\overline{F}_g$ with the averaged interface flux $\overline{F}_\tau(a,b)$ which is the Godunov flux corresponding to the function $\tau = 1/2(f^- + f^+)$. This finite difference scheme is analyzed in [29] and is shown to converge for a large class of fluxes. Numerical experiments comparing this scheme with a Godunov type scheme was reported in [27]. We will also compare this scheme in the numerical experiments in Section 6.

The main objective of this paper is to analyse the upstream mobility flux. It is an adhoc flux for two phase flow in porous media, invented by petroleum engineers from simple physical considerations, and it corresponds to an approximate solution of the Riemann problem. The standard upstream mobility flux for f^- is given by the following formula:

$$\begin{aligned} F^-(a,b) &= \frac{\lambda_1^{-*}}{\lambda_1^{-*} + \lambda_2^{-*}}[q + (g_1 - g_2)\lambda_2^{-*}], \\ \lambda_\ell^{-*} &= \begin{cases} \lambda_\ell^-(a) & \text{if } q + (g_\ell - g_i)\lambda_i^{-*} > 0,\ i = 1,2, i \neq \ell, \\ \lambda_\ell^-(b) & \text{if } q + (g_\ell - g_i)\lambda_i^{-*} \leq 0,\ i = 1,2, i \neq \ell, \end{cases} \quad \ell = 1,2, \end{aligned} \tag{4.5}$$

Similarly, the standard upstream mobility flux corresponding to f^+ can be defined by the following formula,

$$\begin{aligned} F^+(a,b) &= \frac{\lambda_1^{+*}}{\lambda_1^{+*} + \lambda_2^{+*}}[q + (g_1 - g_2)\lambda_2^{+*}], \\ \lambda_\ell^{+*} &= \begin{cases} \lambda_\ell^+(a) & \text{if } q + (g_\ell - g_i)\lambda_i^{+*} > 0,\ i = 1,2, i \neq \ell, \\ \lambda_\ell^+(b) & \text{if } q + (g_\ell - g_i)\lambda_i^{+*} \leq 0,\ i = 1,2, i \neq \ell, \end{cases} \quad \ell = 1,2, \end{aligned} \tag{4.6}$$

These formulas just say that the mobility λ_ℓ must be calculated using the value of the saturation which is upstream with respect to the flow of the phase ℓ since the sign of the quantity $q + (g_1 - g_2)\lambda_2^*$ determines the direction of the flow of phase 1 and the sign of $q + (g_2 - g_1)\lambda_1^*$ determines that of phase 2.

Note that the above formulae are implicit and have been made explicit in [9]. The flux is shown to be Lipschitz, monotone and consistent in the same reference.

As for the Godunov scheme, an interface upstream mobility scheme needs to be defined to take into account the changing rock types. Formulas (4.5),(4.6) can be easily extended to obtain the interface flux $\overline{F}(a,b)$:

$$\begin{aligned}
&\overline{F}(a,b) = \frac{\lambda_1^*}{\lambda_1^*+\lambda_2^*}[q+(g_1-g_2)\lambda_2^*],\\
&\lambda_\ell^* = \begin{cases} \lambda_\ell^-(a) & \text{if } q+(g_\ell-g_i)\lambda_i^* > 0,\ i=1,2, i\neq\ell,\\ \lambda_\ell^+(b) & \text{if } q+(g_\ell-g_i)\lambda_i^* \le 0,\ i=1,2, i\neq\ell, \end{cases} \quad \ell=1,2,
\end{aligned} \tag{4.7}$$

This interface flux preserves the idea of calculating the flux using the phase mobilities which are upstream with respect to the flow of the corresponding phases.

Now we define the upstream mobility flux scheme for a medium with changing rock types as follows,

$$\begin{array}{rcll}
S_1^{n+1} &=& S_1^n - \lambda(F^+(S_1^n,S_2^n) - \overline{F}(S_{-1}^n,S_1^n)),\\
S_j^{n+1} &=& S_j^n - \lambda(F^+(S_j^n,S_{j+1}^n) - F^+(S_{j-1}^n,S_j^n)) & \text{if } j>1,\\
S_{-1}^{n+1} &=& S_{-1}^n - \lambda(\overline{F}(S_{-1}^n,S_1^n) - F^-(S_{-2}^n,S_{-1}^n)),\\
S_j^{n+1} &=& S_j^n - \lambda(F^-(S_j^n,S_{j+1}^n) - F^-(S_{j-1}^n,S_j^n)) & \text{if } j<-1.
\end{array} \tag{4.8}$$

For $S_0 \in L^\infty(\mathbb{R})$ and grid length h and Δt with $\lambda = \frac{\Delta t}{h}$ fixed, define the function $S_h \in L^\infty(\mathbb{R}\times\mathbb{R}_+)$ associated with $\{S_j^n\}$ calculated by the scheme (4.8):

$$S_h(x,t) = S_j^n \quad \text{for } (x,t) \in [x_{j-1/2}, x_{j+1/2}) \times [n\Delta t,\ (n+1)\Delta t), \quad j\neq 0. \tag{4.9}$$

We will analyse the scheme (4.8) in the next section. As for the Godunov case we will need a BV type norm which we define as

$$\begin{aligned}
N_h(f^-,f^+,S_0) &= \sum_{j<-1} |F^-(S_j^0,S_{j+1}^0) - F^-(S_{j-1}^0,S_j^0)| + \sum_{j>1} |F^+(S_j^0,S_{j+1}^0) - F^+(S_{j-1}^0,S_j^0)|\\
&\quad + |\overline{F}(S_{-1}^0,S_1^0) - F^-(S_{-2}^0,S_{-1}^0)| + |F^+(S_1^0,S_2^0) - \overline{F}(S_{-1}^0,S_1^0)|,\\
&\quad N(f^-,f^+,S_0) = \sup_{h>0} N_h(f^-,f^+,S_0).
\end{aligned}$$

5 Convergence Analysis

In this section, we show that the solutions defined by (4.8),(4.9) converge to a weak solution of (2.1) along a subsequence as $h\to 0$. We closely follow the analysis of [2] and will refer to the above paper for details. We first observe that the formulae (4.5), (4.6), (4.7) are implicit. The first step is to make them explicit. For the interior fluxes, this has been done in [9]. We will give an explicit representation of the interface flux. Depending on the ordering of the gravity constants, we have to distinguish the following two cases.

Case 1: $g_1 \le g_2$
Following [9], we define the auxillary quantities for calculating the explicit fluxes

$$\begin{array}{rclcrcl}
\theta_1 &=& q+(g_1-g_2)\lambda_2^-(a), & & \delta_1 &=& q+(g_1-g_2)\lambda_2^*,\\
\theta_2 &=& q+(g_2-g_1)\lambda_1^+(b), & & \delta_2 &=& q+(g_2-g_1)\lambda_1^*.
\end{array}$$

Clearly we have $\theta_1 \leq \theta_2$ and $\delta_1 \leq \delta_2$. We have the following lemma for the explicit formulae of the fluxes,

LEMMA 5.1 *We can have only the following three cases:*

$$\begin{array}{lrcl} 1. & 0 \leq \theta_1 = \delta_1 \leq \theta_2 & \Leftrightarrow & \lambda_1^* = \lambda_1^-(a), \lambda_2^* = \lambda_2^-(a) \\ 2. & \theta_1 = \delta_1 \leq 0 \leq \theta_2 = \delta_2 & \Leftrightarrow & \lambda_1^* = \lambda_1^+(b), \lambda_2^* = \lambda_2^-(a) \\ 3. & \theta_1 \leq \theta_2 = \delta_2 \leq 0 & \Leftrightarrow & \lambda_1^* = \lambda_1^+(b), \lambda_2^* = \lambda_2^+(b) \end{array}$$

The proof is simple and similar to the case of the interior flux F. Details can be found in [26]. This lemma says that just calculating θ_1 and θ_2 is sufficient to determine the upstream side of the flow of each phase.

The other case works in the same way.

Case 2: $g_2 \leq g_1$
We define the auxillary quantities

$$\theta_1 = q + (g_1 - g_2)\lambda_2^+(b), \quad \theta_2 = q + (g_2 - g_1)\lambda_1^-(a)$$

and δ_1 and δ_2 are as in case 1. Now we have $\theta_1 \geq \theta_2$ and $\delta_1 \geq \delta_2$ and the following lemma.

LEMMA 5.2 *We can have only the following three cases*

$$\begin{array}{lrcl} 1. & \theta_1 \geq \theta_2 = \delta_2 \geq 0 & \Leftrightarrow & \lambda_1^* = \lambda_1^-(a), \quad \lambda_2^* = \lambda_2^-(a) \\ 2. & \theta_1 = \delta_1 \geq 0 \geq \theta_2 = \delta_2 & \Leftrightarrow & \lambda_1^* = \lambda_1^-(a), \quad \lambda_2^* = \lambda_2^+(b) \\ 3. & 0 \geq \theta_1 = \delta_1 \geq \theta_2 & \Leftrightarrow & \lambda_1^* = \lambda_1^+(b), \quad \lambda_2^* = \lambda_2^+(b) \end{array}$$

Again calculating θ_1 and θ_2 gives the direction of the flow of each phase and the way to calculate the upstream mobilities. This is easy to implement in a code.

Our goal is to show that the sequence of approximate saturations converges to a weak solution of (2.1). We begin by stating some of the properties of the interface flux.

LEMMA 5.3 *The interface flux $\overline{F}$ as defined in (4.7) is Lipschitz in both its arguments, non decreasing in the first and nonincreasing in the second argument. Furthermore the following also holds*

$$\overline{F}(0,0) = f^-(0) = f^+(0) = 0, \quad \overline{F}(1,1) = f^-(1) = f^+(1) = q.$$

Proof: The proof that the flux is Lipschitz is similar to that for the interior fluxes in [9] and we omit the details. Also the evaluation of $\overline{F}(0,0)$ and $\overline{F}(1,1)$ is easy to check. So let us have a quick pass at the monotonicity properties. We consider for example case 1 i.e. $g_1 \leq g_2$.

If $0 \leq \theta_1 = \delta_1 \leq \theta_2$ we have

$$\lambda_1^* = \lambda_1^-(a), \quad \lambda_2^* = \lambda_2^-(a), \quad 0 \leq \delta_1 = q + (g_1 - g_2)\lambda_2^-(a) \leq \delta_2 = q + (g_2 - g_1)\lambda_1^-(a),$$

$$\overline{F}(a,b) = \frac{\lambda_1^-(a)}{\lambda_1^-(a) + \lambda_2^-(a)}\,\delta_1, \quad \frac{\partial \overline{F}}{\partial a}(a,b) = \frac{(\lambda_1^-)'(a)\lambda_2^-(a)\delta_1 + \lambda_1^-(a)(\lambda_2^-)'(a)(-\delta_2)}{(\lambda_1^-(a) + \lambda_2^-(a))^2}.$$

Since λ_1^-, λ_2^- are both positive functions, λ_1^- is nondecreasing and λ_2^- is nonincreasing, and $0 \leq \delta_1 \leq \delta_2$, we conclude that $\dfrac{\partial \overline{F}}{\partial a}(a,b) \geq 0$ and $\overline{F}(a,b)$ is

nondecreasing with respect to a. Obviously $\overline{F}(a,b)$ does not depend on b so it is nonincreasing with respect to b.

If $\theta_1 = \delta_1 \le 0 \le \theta_2 = \delta_2$ we have

$$\lambda_1^* = \lambda_1^+(b), \quad \lambda_2^* = \lambda_2^-(a), \quad \delta_1 = q + (g_1 - g_2)\lambda_2^-(a) \le 0 \le \delta_2 = q + (g_2 - g_1)\lambda_1^+(b),$$

$$\overline{F}(a,b) = \frac{\lambda_1^+(b)}{\lambda_1^+(b) + \lambda_2^-(a)}\,\delta_1, \ \frac{\partial \overline{F}}{\partial a}(a,b) = \frac{\lambda_1^+(b)(\lambda_2^-)'(a)(-\delta_2)}{(\lambda_1^+(b) + \lambda_2^-(a))^2}, \ \frac{\partial \overline{F}}{\partial b}(a,b) = \frac{\lambda_2^-(a)(\lambda_1^+)'(b)\delta_1}{(\lambda_1^+(b) + \lambda_2^-(a))^2}.$$

Again it is easy to check that $\dfrac{\partial \overline{F}}{\partial a}(a,b) \ge 0$ and $\dfrac{\partial \overline{F}}{\partial b}(a,b) \le 0$. Therefore $\overline{F}(a,b)$ is nondecreasing with respect to a and nonincreasing with respect to b.

If $\theta_1 = \delta_1 \le \theta_2 = \delta_2 \le 0$ we have

$$\lambda_1^* = \lambda_1^+(b), \quad \lambda_2^* = \lambda_2^+(b), \quad \delta_1 = q + (g_1 - g_2)\lambda_2^+(b) \le \delta_2 = q + (g_2 - g_1)\lambda_1^+(b) \le 0,$$

$$\overline{F}(a,b) = \frac{\lambda_1^+(b)}{\lambda_1^+(b) + \lambda_2^+(b)}\,\delta_1, \quad \frac{\partial \overline{F}}{\partial b}(a,b) = \frac{(\lambda_1^+)'(b)\lambda_2^+(b)\delta_1 + \lambda_1^+(b)(\lambda_2^+)'(b)(-\delta_2)}{(\lambda_1^+(b) + \lambda_2^+(b))^2}.$$

Again it is easy to check that $\dfrac{\partial \overline{F}}{\partial a}(a,b) = 0$ and $\dfrac{\partial \overline{F}}{\partial b}(a,b) \le 0$ and $\overline{F}(a,b)$ is nondecreasing with respect to a and nonincreasing with respect to b. ∎

Similar statements for the interior fluxes can be found in [9].

Next, we state the CFL condition for stability of the scheme as the following,

$$\begin{aligned} &\lambda M \le 1, \\ &M = \max\Big\{ \max_{|j|>1,n}\{\frac{\partial F_{j+1/2}^n}{\partial a}(S_j, S_{j+1}) - \frac{\partial F_{j-1/2}^n}{\partial b}(S_{j-1}, S_j)\}, \\ &\qquad \frac{\partial F_{3/2}^n}{\partial a}(S_1, S_2) - \frac{\partial \overline{F}^n}{\partial b}(S_{-1}, S_1), \frac{\partial \overline{F}^n}{\partial a}(S_{-1}, S_1) - \frac{\partial F_{-3/2}^n}{\partial b}(S_{-2}, S_{-1}) \Big\}. \end{aligned} \tag{5.1}$$

This type of a condition was explicitly written out in [25] for the case of one rock type and a slight modification of it gives the result in our case. Then we can prove in a straightforward manner

LEMMA 5.4 *Under the CFL condition (5.1), the upstream mobility scheme defined by (4.8) is monotone.*

We remark that scheme (4.8) is in conservative form, is monotone, but it is not consistent because of the interface flux (some examples are discussed in section 6). Hence, the classical theory (see [11, 22, 14]) does not apply and we have to adopt the analysis presented in [2]. The monotonicity of the scheme leads to the following discrete L^1 contractivity result:

LEMMA 5.5 *Let $S_0, \in L^\infty(\mathbb{R},\ [0,1])$ be the initial data, and let $\{S_j^n\}$ be the corresponding solution calculated by the upstream mobility flux scheme* (4.8)*. then,*

$$\sum_{j\neq 0} |S_j^{n+1} - S_j^n| \le \sum_{j\neq 0} |S_j^n - S_j^{n-1}|. \tag{5.2}$$

Proof: As the scheme (4.8) is monotone and conservative, this estimate follows by applying the Crandall-Tartar lemma (see [14]). ∎

The next step is to obtain estimates in L^∞ for the approximate solutions. For Monotone, Consistent and Conservative schemes , such estimates follow from a discrete maximum principle. But for the scheme (4.8), the lack of consistency implies that the discrete maximim principle is no longer true. Instead, as in [2], we can use the consistency of the interface flux at the points 0 and 1 to obtain that $[0,1]$ is an invariant region for the scheme and obtain the following lemma,

LEMMA 5.6 *Let $S_0 \in L^\infty(\mathbb{R},[0,1])$ be the initial data, and let $\{S_j^n\}$ be the corresponding solution calculated by the finite volume scheme* (4.8)*. The following holds,*

$$0 \leq S_j^n \leq 1 \quad \forall j,n. \tag{5.3}$$

Proof. Since $0 \leq S_0 \leq 1$, hence for all j, $0 \leq S_j^0 \leq 1$. By induction, assume that (5.3) holds for n. Then from Lemma 5.3 we have

$$\begin{aligned}
0 &= H_{-1}(0,0,0) \leq H_{-1}(S_{j-1}^n, S_j^n, S_{j+1}^n) = S_1^{n+1} \leq H_{-1}(1,1,1) = 1 \text{ if } j \leq -2,\\
0 &= H_1(0,0,0) \leq H_1(S_{j-1}^n, S_j^n, S_{j+1}^n) = S_j^{n+1} \leq H_1(1,1,1) = 1 \quad \text{if } j \geq 2,\\
0 &= H_{-2}(0,0,0) \leq H_{-2}(S_{-2}^n, S_{-1}^n, S_1^n) = S_{-1}^{n+1} \leq H_{-2}(1,1,1) = 1,\\
0 &= H_2(0,0,0) \leq H_2(S_{-1}^n, S_1^n, S_2^n) = S_1^{n+1} \leq H_2(1,1,1) = 1.
\end{aligned}$$

This proves (5.3). ∎

As pointed out earlier, the key difficulty in the convergence analysis is to obtain BV type estimates on the approximations. For a monotone, consistent and conservative scheme, such estimates following from the discrete L^1 contractivity and the translation invariance (see [14]). But in this case, the scheme is not consistent and we cannot expect the approximate solutions to be uniformly bounded in BV. Rather, the difficulty is circumvented by using the singular mapping technique first introduced by Temple in [28] and adapted for schemes for single conservation laws by Towers in [29]. The singular mapping was also adopted in the convergence proof in [2]. More recently, several modifications of the singular mapping have been suggested in [27], [3] etc.

The central idea in using the singular mapping technique is to estimate the total variation of the approximate solutions under the singular mapping by the variation of the fluxes in neighboring cells and use the discrete L^1 contractivity. This method works well for upwind schemes like Godunov and Enquist Osher but it does not work for other types of numerical fluxes like the Lax-Friedricks flux. The same is true for the upstream mobility flux and we have to adapt the technique to work in this case. We do so by using the idea of chain estimates like in [4] . We start by defining the singular mappings. ,we use the following standard notation $a \in \mathbb{R}$, then $a_+ = \max\{a,0\}, a_- = \min\{a,0\}, a = a_+ + a_-, |a| = a_+ - a_-$.
The singular mappings are given by,

$$\psi_1(\theta) = \int_\alpha^\theta |f^{-\prime}(\xi)| d\xi, \quad \psi_2(\theta) = \int_\alpha^\theta |f^{+\prime}(\xi)| d\xi \tag{5.4}$$

where $\alpha \in [0,1]$ is some number. Note that we use the same form of singular mappings as in [2] expect that there are centerered at an arbitrary point as in [27]. Now we are in a position to define the transformed schemes for the discrete values of the solution. We define them as

$$z_j^n = \begin{cases} \psi_1(S_j^n) & \text{if} \quad j \leq -1 \\ \psi_1(S_{-1}^n) & \text{if} \quad j \geq -1 \end{cases}, w_j^n = \begin{cases} \psi_2(S_1^n) & \text{if} \quad j \leq 1 \\ \psi_2(S_j^n) & \text{if} \quad j \geq 1 \end{cases}.$$

Like in [27], we define two sets of transformed variables which enables us to simplify the proof to some extent as compared to [2]. Our goal is to estimate the variation of the transformed scheme at each time level. For simplicity, let us suppres the subscript n as we are dealing with the same time level. Then

$$TV(z_j) = \sum_{j \neq 0} |z_j - z_{j+1}| = 2 \sum_{j \neq 0} (z_j - z_{j+1})_+$$

In [2],[27], this variation was controlled individually in each cell by the flux variation across the neighboring cells. For details see lemma (5.4) in [27]. But such an estimate relied on the upwind nature of the Godunov flux and is not necessarily true for the upstream mobility flux as the upstream mobility flux gives different answers from the Godunov and Enquist-Osher fluxes when the phases are flowing in different directions. Rather, nonlocal variation estimates hold in this case as will be explained below. For this, we observe from the definition of the singular mapping (5.4) that $(z_j - z_{j+1})_+ > 0$ if and only if $S_j > S_{j+1}$. Same observation also applies to w_j's. We use this ordering of the neighboring cell values to define the following,
Define $\underline{J} = \{j \leq -2\}$ and we define some subsets of this set as follows,
Definition: $\underline{I} \subset \underline{J} = \{i \in \underline{J} : S_i < S_{i+1}\}$ is the set of admissble indices.
Note that this implies that for each $i \in \underline{I}$, there exists a unique $k(i)$ such that the following holds,
1. $S_i \leq S_{i-1} \leq \ldots \leq S_{i-k(i)}$
2. $S_{i-k(i)-1} < S_{i-k(i)}$
We denote the following,
1.$k(i) = 0$ if $S_{i-1} < S_i$ and
2.$k(i) = \infty$ if $\forall j < i, \quad S_j \geq S_{j+1}$
So there can be atmost one $i \in \underline{I}$ such that $k(i) = \infty$. Let i_0 be such that $i_0 = \min_{\underline{I}} i$. Note that i_0 is not necessarily equal to -2. Now we can define a chain as $\underline{J}_i = \{j : k(i) \leq j \leq i\}$. With the above definitions, it easy to check that $\underline{J} = \cup_{i \in \underline{I}} \underline{J}_i$.

Similarly denote, $\overline{J} = \{j \geq 1\}$ and we define some subsets of this set as follows,
Definition: $\overline{I} \subset \overline{J} = \{i \in \overline{J} : S_i < S_{i+1}\}$ is the set of admissble indices.
Note that this implies that for each $i \in \overline{I}$, there exists a unique $k(i)$ such that the following holds,
1. $S_i \geq S_{i+1} \geq \ldots \geq S_{i+k(i)}$
2. $S_{i+k(i)+1} > S_{i+k(i)}$
We denote the following,
1.$k(i) = 0$ if $S_{i+1} > S_i$ and
2.$k(i) = \infty$ if $\forall j > i, \quad S_j \geq S_{j+1}$
So there can be atmost one $i \in \overline{I}$ such that $k(i) = \infty$. We denote the minimum

value in $\overline{I}$ to be i^0. Now we can define a chain as $\overline{J}_i = \{j : i \leq j \leq k(i)\}$. With the above definitions, it easy to check that $\overline{J} = \cup_{i \in \overline{I}} \overline{J}_i$.
Equipped the definitions above, we are in a position to state the main lemma of this section in the following,

LEMMA 5.7 *$\forall i \in \underline{I}$, the following estimates hold, if $i < -2$ and $k(i) \neq \infty$ then,*

$$\begin{aligned} \sum_{j \in \underline{J}_i} (z_j - z_{j+1})_+ &\leq \sum_{j \in \underline{J}_i} \{|F^-(S_j, S_{j+1}) - F^-(S_{j-1}, S_j)| \\ &+ |F^-(S_{j+1}, S_{j+2}) - F^-(S_j, S_{j+1})|\} \end{aligned} \tag{5.5}$$

for i_0 as defined above, and such that $i_0 = -2$, we have the following estimate,

$$\sum_{j \in \underline{J}_{i_0}} (z_j - z_{j+1})_+ \leq 2M \tag{5.6}$$

In case, i happens to be the only index such that $k(i) = \infty$, then

$$\sum_{j \in \underline{J}_i} (z_j - z_{j+1})_+ \leq 2M \tag{5.7}$$

Similarly, if $i \in \overline{I}$ and $k(i) \neq -\infty$, then the following estimate holds

$$\begin{aligned} \sum_{j \in \overline{J}_i} (w_j - w_{j+1})_+ &\leq \sum_{j \in \overline{J}_i} \{|F^+(S_j, S_{j+1}) - F^+(S_{j-1}, S_j)| \\ &+ |F^+(S_{j+1}, S_{j+2}) - F^+(S_j, S_{j+1})|\} \end{aligned} \tag{5.8}$$

for i^0 as defined above, and such that $i^0 = 1$, we have the following estimate,

$$\sum_{j \in \overline{J}_{i^0}} (z_j - z_{j+1})_+ \leq 2M \tag{5.9}$$

And in case i is such that $k(i) = \infty$, then we have that

$$\sum_{j \in \overline{J}_i} (w_j - w_{j+1})_+ \leq 2M \tag{5.10}$$

Proof: We will only provide proofs for the estimates (5.5) and (5.7). The other inequalities follow in the same manner. We have to consider three separate cases to check the estimate namely,
Case 1: $0 \leq S_{k(i)} \leq \theta^-$.
In this case, it follows from the L^∞ bounds and the definitions that $0 \leq S_i \leq \ldots \leq S_{k(i)} \leq \theta^-$. Hence, one can check that

$$\sum_{j \in \underline{J}_i} (z_j - z_{j+1})_+ = f^-(S_{k(i)}) - f^-(S_i) \tag{5.11}$$

From the definition of $\underline{I}$, we get that $S_i \leq S_{i+1}$ and $S_{k(i)+1} \leq S_{k(i)}$. Therefore, using the monotonicity and consistency of the interior upstream mobility flux scheme,we get that

$$F^-(S_i, S_{i+1}) \leq F^-(S_i, S_i) = f^-(S_i) \tag{5.12}$$

and

$$F^-(S_{k(i)}, S_{k(i)+1}) \geq F^-(S_{k(i)}, S_{k(i)}) = f^-(S_{k(i)}) \tag{5.13}$$

Therefore by combining the above estimates, we get that

$$\begin{aligned} f^-(S_{k(i)}) - f^-(S_i) &= f^-(S_{k(i)}) - F^-(S_{k(i)+1}, S_{k(i)+2}| \\ &+ F^-(S_{k(i)+1}, S_{k(i)+2}) - \dots \\ &+ \dots - F^-(S_{i-1}, S_i) \\ &+ F^-(S_{i-1}, S_i) - f^-(S_i) \end{aligned}$$

Now by using (5.12) and (5.13), we get that ,

$$\sum_{j \in \underline{J}_i} (z_j - z_{j+1})_+ \leq \sum_{j \in \underline{J}_i} |F^-(S_j, S_{j+1}) - F^-(S_{j-1}, S_j)|$$

thus proving (5.5). Next we consider,
Case 2: $\theta^- \leq S_i \leq 1$.
In this case, it follows from the L^∞ bounds and the definitions that $\theta^- \leq S_i \leq \dots \leq S_{k(i)} \leq 1$. Hence, one can check that

$$\sum_{j \in \underline{J}_i} (z_j - z_{j+1})_+ = f^-(S_i) - f^-(S_{k(i)}) \tag{5.14}$$

From the definition of $\underline{I}$, we get that $S_i \leq S_{i-1}$ and $S_{k(i)-1} \leq S_{k(i)}$. Therefore, using the monotoniticity and consistency of the interior upstream mobility flux scheme,we obtain

$$F^-(S_{i-1}, S_i) \geq F^-(S_i, S_i) = f^-(S_i) \tag{5.15}$$

and

$$F^-(S_{k(i)-1}, S_{k(i)}) \leq F^-(S_{k(i)}, S_{k(i)}) = f^-(S_{k(i)}). \tag{5.16}$$

Therefore by combining the above estimates, we have

$$\begin{aligned} f^-(S_{k(i)}) - f^-(S_i) &= f^-(S_{k(i)}) - F^-(S_{k(i)+1}, S_{k(i)+2})| \\ &+ F^-(S_{k(i)+1}, S_{k(i)+2}) - \dots \\ &+ \dots - F^-(S_{i-1}, S_i) \\ &+ F^-(S_{i-1}, S_i) - f^-(S_i) \end{aligned}$$

Now by using (5.15) and (5.16), we get

$$\sum_{j \in \underline{J}_i} (z_j - z_{j+1})_+ \leq \sum_{j \in \underline{J}_i} \{|F^-(S_j, S_{j+1}) - F^-(S_{j-1}, S_j)|$$

thus proving (5.5).
Case 3:$S_i \leq \theta^- \leq S_{k(i)}$
In this case, $\exists \quad l(i) \in \underline{J}_i$ such that $S_i \leq \dots \leq S_{l(i)} \leq \theta^- \leq S_{l(i)-1} \leq \dots \leq S_{k(i)}$. We get that

$$\sum_{j \in \underline{J}_i} (z_j - z_{j+1})_+ = f^-(\theta^-) - f^-(S_{k(i)}) + f^-(\theta^-) - f^-(S_i) \tag{5.17}$$

Again by the monotonicity and consistency of the interior fluxes, we have the following estimate,

$$F^-(S_{l(i)-1}, S_{l(i)}) \geq F^-(\theta^-, \theta^-) = f^-(\theta^-) \tag{5.18}$$

Therefore, from the estimates (5.17), (5.18), (5.12) and (5.16), we have

$$\begin{aligned} f^-(\theta^-) - f^-(S_i) &= f^-(\theta^-) - F^-(S_{l(i)}, S_{l(i)+1} \\ &+ F^-(S_{l(i)}, S_{l(i)+1}) - \dots \\ &+ \dots - F^-(S_{i-1}, S_i) \\ &+ F^-(S_{i-1}, S_i) - f^-(S_i) \end{aligned}$$

and

$$\begin{aligned} f^-(\theta^-) - f^-(S_{k(i)}) &= f^-(\theta^-) - F^-(S_{l(i)-2}, S_{l(i)-1}) \\ &+ F^-(S_{l(i)-2}, S_{l(i)-1}) - \dots \\ &+ \dots - F^-(S_{k(i)}, S_{k(i)+1}) \\ &+ F^-(S_{k(i)}, S_{k(i)+1}) - f^-(S_{k(i)}) \end{aligned}$$

Combining the above 2 estimates, we get the desired inequality and prove (5.5) in all the 3 cases. Next, we prove (5.7). In case of i being the unique element of $\underline{I}$ such that $k(i) = \infty$. It is easy to from the L^∞ and Lipschitz bounds that

$$\begin{aligned} \sum_{-\infty}^{i} (z_j - z_{j+1})_+ &\leq f(\theta^-) - f^-(u_i) \\ &+ f^-(\theta^-) - f^-(1) \\ &\leq M(|\theta^- - 1| + \theta^-) = M \end{aligned}$$

Thus we have the estimate (5.7). The other estimates can be proved similarly. ∎

We use the above inequalities to show the following variation bound on the singular mapping,

LEMMA 5.8 *The transformed sequences are of bounded total variation and the following estimate holds,*

$$\max\{TV(z_j^n), TV(w_j^n)\} \leq \frac{4}{\lambda} N(f^-, f^+, S_0) + 2M \tag{5.19}$$

Proof: We provide a proof for the sequence $\{z_j^n\}$, the other bound follows in a similar way.We

$$\begin{aligned} TV(z_j^n) &= 2(\sum_{j\in\mathbb{Z}} (z_j^n - z_{j+1}^n)_+) \\ &= \sum_{j\in\underline{J}} (z_j^n - z_{j+1}^n)_+ \\ &= \sum_{i\in\underline{I}} \sum_{j\in\underline{J_i}} (z_j^n - z_{j+1}^n)_+ + 2M \end{aligned} \tag{5.20}$$

By adding the chain inequalities (5.5), 5.6 and 5.7), we get that

$$\begin{aligned}\sum(z_j^n - z_{j+1}^n)_+ &= 2(\sum_{j\le -2}|G(u_j^n,u_{j+1}^n) - G(u_{j-1}^n,u_j^n)| + |G(u_{-2}^n,u_{-1}^n - \overline{F}(u_{-1}^n,u_1^j)| \\ &+ |\overline{F}(u_{-1}^n,u_1^j) - F(u_1^n,u_2^n)| + \sum_{j\ge 2}|F(u_j^n,u_{j+1}^n) - F(u_{j-1}^n,u_j^n)| + 2M \\ &= \frac{2}{\lambda}\sum_{j\neq 0}|u_j^{n+1} - u_j^n| + 4M \end{aligned} \tag{5.21}$$

Now by using the discrete L^1 contractivity, we get the desired estimate. In a similar way, we can get the total variation bound for $\{w_j^n\}$ and complete the proof of the lemma. ∎

In order to show convergence of solutions generated by the scheme, we need to define the following piecewise constant functions,Let z^h, w^h be defined as $z^h(x,t) = z_j^n, w^h(x,t) = w_j^n, \quad \forall \quad (x,t) \in I_j^n$. We translate the bounds on the discrete values in terms of the above functions in the following lemmas which we state without proof (for a proof see [27]).

LEMMA 5.9 *With the functions defined as above and $\forall t \in \mathbb{R}_+$,we have,*

$$\max\{TV(z^h), TV(w^h)\} \quad \le \quad \frac{4}{\lambda}N_h(f^-,f^+,u_0) + 4M \tag{5.22}$$

LEMMA 5.10 *Let $S_0 \in L^\infty(\mathbb{R},[0,1])$ such that $N(f^-,f^+,S_0) < \infty$ be initial data and let S_h be the co rresponding solutions obtained by the scheme (2.1),then*

$$0 \le S_h(x,t) \le 1 \qquad \forall \ (x,t) \in \mathbb{R}\times\mathbb{R}_+ \tag{5.23}$$

$$\int_{\mathbb{R}} |S_h(x,t) - S_h(x,\tau)|dx \quad \le \quad N_h(f^-,f^+,S_0)(2\Delta t + |t-\tau|) \tag{5.24}$$

We are in a position to state our main convergence theorem. The key step was to prove the total variation bounds on the singular mappings and the fact that the singular mapping is monotone and hence invertible. We have that

THEOREM 5.1 *Assume that the CFL condition is satisfied and the initial data S_0 satisfies the hypothesis IN_1 and IN_2, Let S_h be approximate solutions defined above,then there exists a subsequence (still denoted by h) such that S_h converge almost everywhere to a weak solution S of (2.1).In fact $S_h \to S$ in $L^\infty_{\rm loc}(\mathbb{R}_+, L^1_{\rm loc}(\mathbb{R}))$ as h goes to 0. Furthermore, the limit solution satisfies the interior entropy condition (3.2).*

Proof:This is the main convergence theorem for the upstream mobility flux scheme (4.8). The proof follows by the classical arguments of the Lax-Wendroff theorem (See [14]) and the modifications introduced in [2]. We omit the details and refer to the above quoted paper for them.

For any fixed $t > 0$,we have the BV bounds from the Lemma (5.9) and by using the standard Rellich compactness theorem that upto subsequences (still

denoted by h),we get that $z_h(.,t), w_h(.,t)$ converge in L^1 and for almost all x to $z(.,t)$ and $w(.,t)$ respectively.

For fixed t and for almost all $x < 0$, then from the convergence we have that $\psi(S_h) \to z$. Note that ψ is monotone for $x < 0$ and we get that $S_h(x,t) \to \psi^{-1}(z(x,t)) = S(x,t)$. Thus for all $x < 0$,we get that $S_h(.,t)$ converges to $S(.,t)$ for almost all $x < 0$.Similarly,for $x > 0$,we define $S(x,t) = \psi_2^{-1}(z_h(x,t)$ and get the a.e convergence.Now we use the standard density argument along with the time continuity estimate (5.10),to get that

$$S_h \to S \quad \in L^\infty_{\text{loc}}((0,T), L^1_{\text{loc}}(\mathbb{R})) \tag{5.25}$$

Once we have the above convergence, we can use the standard arguments of the Lax-Wendroff type in order to show that S_h converges to a weak solution of (2.1).The proof follows exactly as in [27] and we refer the reader to this reference for details. Similarly, the consistency of the scheme with the interior entropy condition is shown by using the numerical entropy fluxes of Crandall-Majda (see [14]). Check [2] for the details. ∎

6 Entropy consistency of the scheme

In the previous sections, we have shown that the upstream mobility flux scheme is well defined for two-phase flow in an heterogenous medium with two rock types and that it generates solutions which converge to weak solutions of the conservation law (2.1) and satisfy interior Kruzkhov type entropy condition. But, for the solutions of the scheme to be admissible, we have to show that they also satisfy the interface entropy condition (3.3). As pointed out earlier, we remark that this entropy condition is pointwise and essentially amounts to the exclusion of undercompressive waves at the interface ($x = 0$). In ([2]), it was shown that the Godunov type scheme (4.3) satifies the interface entropy condition by means of a contradiction argument. In this section, we investigate the question of whether the limit solution generated by the upstream mobility flux scheme also satisfies this interface entropy condition or not.

It will be shown by means of various numerical experiments that the limit solution generated by scheme (4.8) which uses the upstream mobility flux need not satisfy the interface entropy condition and counterexamples are given. In other cases that we report, it is far from clear whether the interface entropy condition is actually satisfied. In fact, the numerical evidence suggests that this condition is not satisfied in the pointwise sense as required in the entropy theory of ([2]) on account of certain boundary layer phenomena at the interface although the entropy condition may be satisfied in a weaker integral sense.

It is worth mentioning that there are several entropy theories for equations of the type (2.1) like those presented in [2] and in [19]. It will be shown that in some cases, the solutions generated by the scheme (4.8) satisfy the entropy conditions of [19] and in some other cases, the conditions of [2].

We will now present the five numerical experiments illustrating five different situations.

Experiment 1

In this example, we consider the flux functions given by,

$$\begin{array}{lcllcl} \lambda_1^+(S) & = & 1.1S & \lambda_2^+(S) & = & 1.1(1-S) \\ \lambda_1^-(S) & = & S & \lambda_2^-(S) & = & 1-S \\ g_1 & = & 2 & g_2 & = & 1 \\ \phi & = & 1 & q & = & 0 \end{array}$$

As is clear from the above, we are considering that the porosity and the relative permeabilities dont change across the rock types and the absolute permeabilities only change with $K^+ = 1.1$ and $K^- = 1$. The shape of the corresponding fluxes f^- and f^+ are shown in Fig. 6.

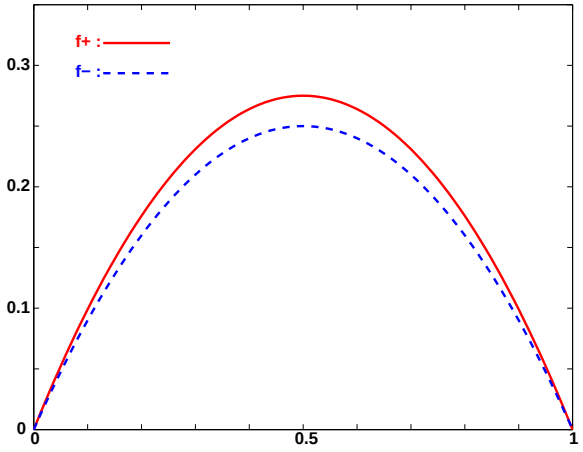

Figure 6.1: Flux functions in experiment 1

We consider for initial data, $S_0(x) = \begin{cases} 0.65 & \text{if} \quad x < 0 \\ 0.35 & \text{if} \quad x > 0. \end{cases}$ In this case, since the flux functions do not intersect in the interior of the interval (0.1), the entropy solution in this case coincides for the entropy theories of [2] and [19] and consists of a rarefaction fan joining 0.65 and 0.5 on the left and a steady discontinuity at the interface with 0.5 as the left trace and 0.35 as the right trace. Note that the entropy solution does not admit underconmpressive waves at the interface as $f^{-\prime}(0.5) \equiv 0$.

We present the solutions obtained by the Godunov type finite difference scheme which we term as the Exact Riemann Solver (ERS) and the Upstream Mobility scheme which we term as UM. Also, we compute solutions with the staggered mesh version of the Godunov scheme developed by Towers in [29] and [30]. We term this scheme as AV. The computed solutions are shown at two different times and for two different mesh sizes in Fig. 6.2 and Fig. 6.3.

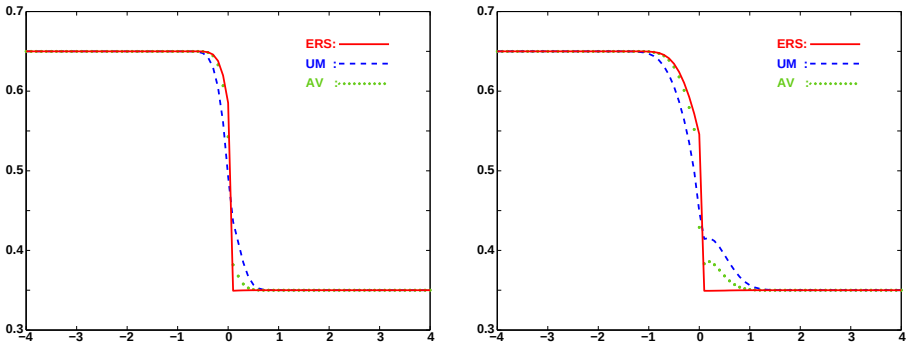

Figure 6.2: Solutions in experiment 1 with h = 0.1 at times t=0.5 and t=1.5

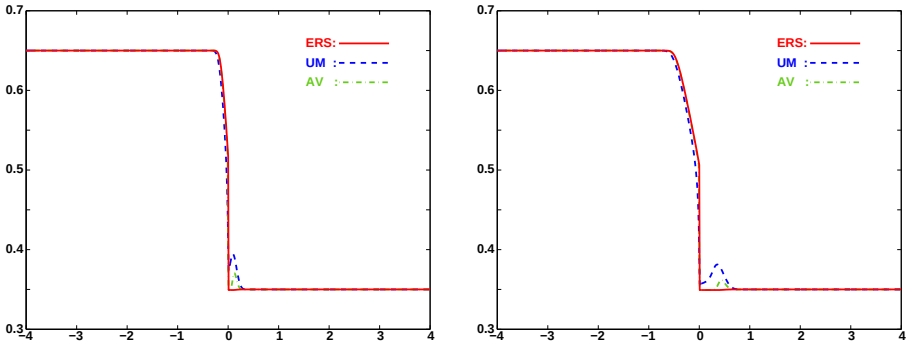

Figure 6.3: Solutions in experiment 1 with h = 0.01 at t=0.5 and t=1.5

In Figure 6.2, we show the numerical results obtained with the mesh size $h = 0.1$ and the CFL constant $\lambda = \frac{1}{8}$. As expected at this rather large mesh size, the resolution is not high although the ERS is already giving very good results with the interface discontinuity being resolved perfectly. On the other hand, both UM and AV do not resolve the interface discontinuity well. In fact, as seen in Fig. 6.2, the left trace of the solution as computed by UM is approximately 0.4 which is less than the expected trace of 0.5. This is indicative of the development of a boundary layer at the interface $x = 0$. Another anomaly is the existence of a travelling wave in both UM and AV that is clearly unphysical as the solution is constant 0.35 in $x > 0$. The amplitude of this spurious wave is higher for UM than for AV. Both these phenomena indicate that we cannot prove that the limit solution generated by UM and AV are consistent with the interface entropy condition (3.3) in a pointwise sense.

In order to confirm the above proposition, we reduce the mesh size to $h = 0.01$ and show the solution in Fig. 6.3. Again, we see that ERS resolves both the rarefaction and the interface discontinuity very well with little numerical diffusion whereas both UM and AV do not match the solution. Even with a very small mesh size, the left trace at the interface of the solution computed with UM is around 0.4 and is well below the required value of 0.5. Also, the spurious travelling wave seen before is still present although its magnitude has decreased. As stated earlier, the existence of both a boundary layer and a

travelling wave forces us to believe that the solution computed with UM is not consistent with the interface entropy condition. The same holds true for the solutions computed by AV.

The first numerical experiment that we have presented represents the simplest type of discontinuity at the interface involving only a change in the absolute permeability across the interface. Even in this simple situation, the UM flux scheme does not perform as well as ERS and the limit solution obtained by it doesnot seem to satisfy the interface entropy condition of [2]. Hence, more interesting and complicated behaviour is expected when we consider changes in relative permeabilities across the interface. As will be shown in the coming numerical experiments, the limit solution computed by UM will converge to the entropy solution of [2] in some cases and the entropy solution of [19] in some other cases.

We start with an example where the solution given by UM seems to converge to the entropy solution of [2] in the following numerical experiment,

Experiment 2

In this experiment, we consider the following flux functions and parameters,

$$\begin{array}{llllll} \lambda_1^+(S) & = & S & \lambda_2^+(S) & = & 2(1-S) \\ \lambda_1^-(S) & = & 2S & \lambda_2^-(S) & = & 1-S \\ g_1 & = & 2 & g_2 & = & 1 \\ \phi & = & 1 & q & = & 0 \end{array}$$

In this case, we are changing the relative permeability functions across the interface. The flux functions are shown in Fig. 6.

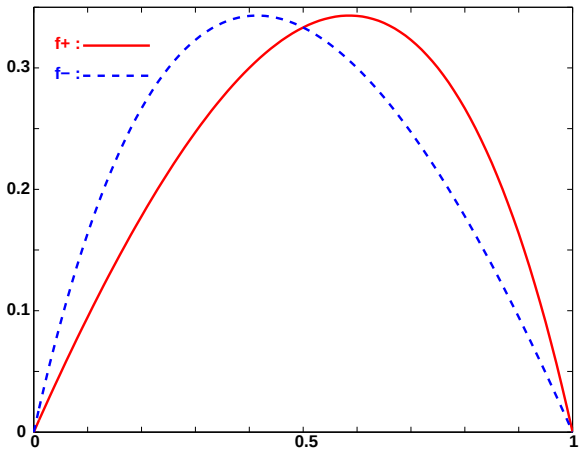

Figure 6.4: Flux functions in experiment 2

Observe that in this case, the flux functions intersect at the point 0.5 in the interior of the domain and the point of intersection is undercompressive i.e $f^{+\prime}(0.5) > 0$ and $f^{-\prime}(0.5) < 0$. The initial data are $S_0(x) = 0.5 \quad \forall \quad x \in \mathbb{R}$, so we start with a state where the light and heavy phases are fully mixed. In this case, the entropy solution of [2] is given by the constant state 0.5 connected to

the left trace 0.42 by a rarefaction fan on the left and the constant state 0.5 connected to the right trace 0.58 on the right. Observe that this solution satisfies the interface entropy condition (3.3) as $f^{-\prime}(0.42) = 0$ and $f^{+\prime}(0.58) = 0$.

As the flux functions satisfy the "crossing" condition of [19], we can apply the Kruzkhov type condition of [19] to get that their entropy solution in this case is given by $S \equiv 0.5$. This implies that there is no flow in the medium which is unnatural as noticed in [21]. This is one situation where the above entropy theories differ and the entropy theory of [2] captures the physically relevant solution. We have computed the solutions using all the three schemes to obtain the results as shown in Figures 6.5 and 6.6. Fig. 6.5) shows the solutions obtained by schemes ERS, UM and AV with $h = 0.1$ and the CFL parameter $\lambda = 0.125$. We show the computed solutions at times $t = 1.5$ and $t = 3$ respectively. As can be observed in Fig. 6.5, the solution obtained by AV is the constant state 0.5 in accordance with the entropy theory of [19]. The solution computed by ERS converges towards the entropy solution as discussed above with a good resolution of the interface discontinuity and some numerical diffusion at the rarefactions. The solution obtained by UM shows the same qualitative behaviour as that calculated by ERS although the left trace is 0.35 which is well below the left trace of the solution i.e 0.42. Similarly the right trace of the UM solution is 0.65 which is above the required right trace of 0.58. This is again indicating the evidence for UM of a numerical boundary layer at the interface which was noticed in experiment 1.

In order to get a better estimate of the boundary layer, we shrink the mesh size to $h = 0.01$ and present the results in Fig. 6.6.

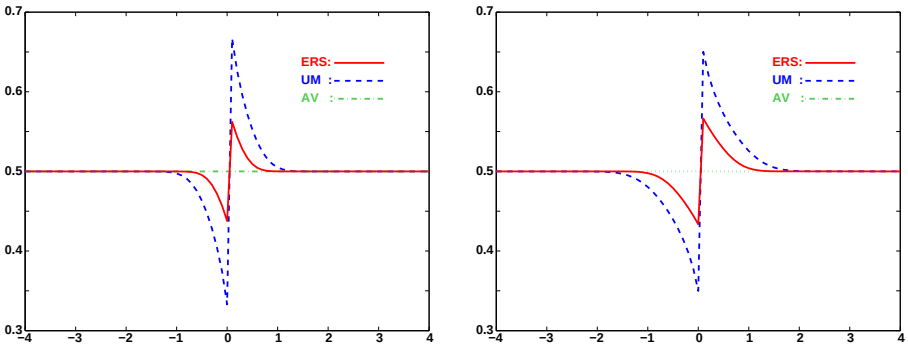

Figure 6.5: Solutions in experiment 2 with h=0.1 at t=1.5 and t=3

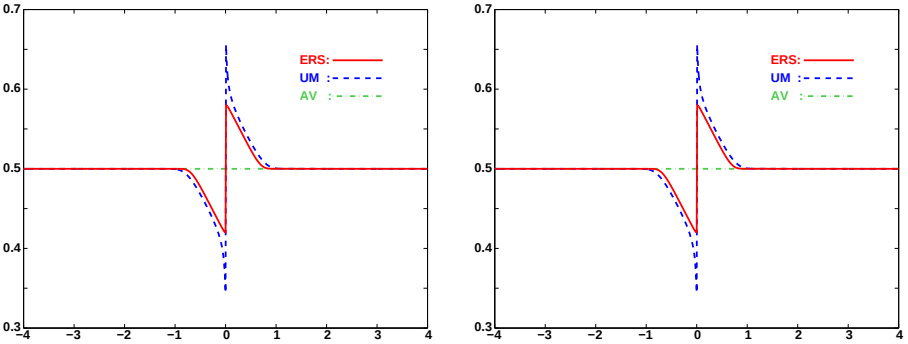

Figure 6.6: Solutions in experiment 2 with h = 0.01 at t=1.5 and t=3

Again, the solution obtained by AV is the constant state 0.5. As expected given the convergence results presented before, the solution obtained by ERS is almost exact. Notice that the left and right traces at $x = 0$ are exactly 0.42 and 0.58 as in the exact solution of this Riemann problem showing the high resolution of the scheme. The qualitative behaviour of the solution obtained by UM is again similar to that of ERS. But the boundary layer at the interface remains as the left trace is still below 0.35 (well below 0.42) and the right trace is still above 0.65 well above the required right trace of 0.58. This suggests to us that the boundary layer remains intact as $h \to 0$ and the traces at the interface are different from the expected traces, although, the width of this boundary layer shrinks with a reduction in the mesh size. This suggests that the limit solution obtained by UM converges to the entropy solution of [2] in an integral sense.

In experiment 2, we considered flux functions where the solutions obtained by UM converged to the entropy solution of [2] in an integral sense. The crucial point of the previous experiment was that the fluxes intersect in the interior of the interval (0,1) and the point of intersection was undercompressive. Next, we consider a situation of the similar type where solutions computed by UM seem to behave very differently.

Experiment 3 In this experiment we consider the flux functions and parameters given by,

$$\begin{array}{lcllcl} \lambda_1^+(S) & = & S & \lambda_2^+(S) & = & (1-S^2) \\ g_1 & = & 2 & g_2 & = & 1 \\ \phi & = & 1 & q & = & 0 \end{array}$$

$$\begin{array}{lcll} \lambda_1^-(S) & = & 1.75S & \text{if } S \le 0.25 \\ & = & 0.25S + 0.375 & \text{if } S \ge 0.25 \\ \lambda_2^- & = & 1 - S^2 & \end{array}$$

The flux functions are schown in Fig. 6. Notice that in this case, f^- and f^+ intersect at 0.5 and the intersection is undercompressive. This is a situation which looks similar to that of the previous numerical experiment.

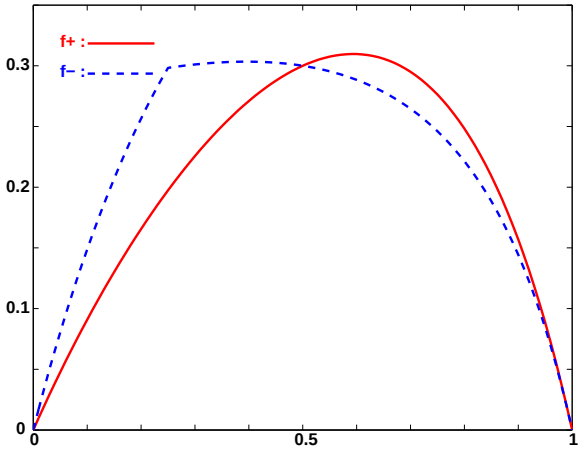

Figure 6.7: Flux functions in experiment 3

Again we start with the constant initial data given by $S_0(x) = 0.5 \quad \forall \quad x \in \mathbb{R}$.

As in experiment 2, the entropy solution of [2] consists of the constant state 0.5 connected to the left trace 0.45 by a rarefaction on the left, a steady discontinuity at $x = 0$ connecting the left trace 0.45 to the right trace 0.54,and the constant state 0.54 being connected by another rarefaction to the constant state 0.5 on the right. As the "crossing condition" is satisfied, the entropy solution of [19] is just the constant $S \equiv 0.5$. We show in figure (6.8) the results obtained by all three schemes with $h = 0.1$ and the CFL $\lambda = 0.125$.

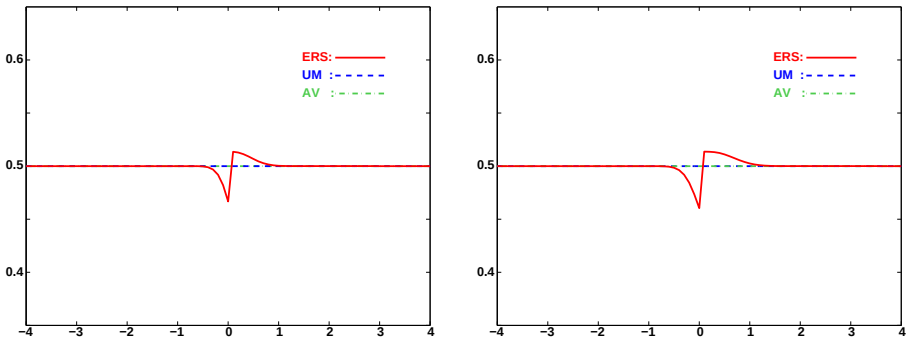

Figure 6.8: Solutions in experiment 3 with h = 0.1 at t=2.5 and t=3.75

As noticed in Fig. 6.8, the solution computed by ERS approximates the entropy solution of [2] while the solution computed by AV is the constant 0.5. But what is really surprising is that the solution computed by UM is also the constant 0.5. In fact, this example has been constructed in such a way that $\lambda_1^-(0.5) = \lambda_1^+(0.5)$ and $\lambda_2^-(0.5) = \lambda_2^+(0.5)$. Hence from the very definition of the upstream mobility flux, it is easy to check that the solution computed by UM remains the constant 0.5 at all time steps.

Thus so far we have shown two experiments involving fluxes with an undercompressive intersection in which the entropy solutions of [2] and [19] differ. In experiment 2, the solutions computed by UM flux seems to converge to the entropy solution of [2] in an integral sense, though not pointwise whereas, in experiment 3, the UM flux gives the constant solution which has been considered in literature as unphysical (see [21]) and converges to the entropy solution of [19]. Despite similar flux geometry, this inconsistent behaviour of the UM flux indicates the difficulties of characterizing the limit solutions computed by the scheme.

The above numerical experiments clearly show that the inconsistent behaviour of the UM flux when the fluxes intersect in the interior of the interval (0,1) and the point of intersection is undercompressive. We now investigate another type of flux geometry in which the flux functions intersect and the point of intersection is overcompressive. In this case, the limit solution obtained with the UM flux also shows an inconsistent entropy behaviour.

Experiment 4 In this experiment, we consider the following flux functions and parameters,

$$\begin{array}{llllll} \lambda_1^+(S) & = & 2S & \lambda_2^+(S) & = & (1-S) \\ \lambda_1^-(S) & = & S & \lambda_2^-(S) & = & 2(1-S) \\ g_1 & = & 2 & g_2 & = & 1 \\ \phi & = & 1 & q & = & 0 \end{array}$$

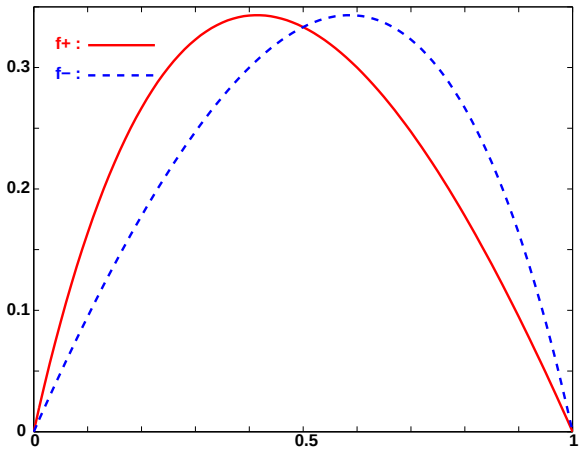

Figure 6.9: Flux functions in experiment 4
.eps

The flux functions are shown in Fig. 6. Observe that f^- and f^+ intersect at 0.5 and that the intersection is overcompressive i.e $f^{-\prime}(0.5) > 0$ and $f^{+\prime}(0.5) < 0$. We consider the initial data $S_0(x) = \begin{cases} 2/3 & \text{if} \quad x < 0 \\ 1/3 & \text{if} \quad x > 0. \end{cases}$

The entropy solution of [2] in this case consists of the constant state 0.66 connected by a rarefaction to the left trace 0.58 on the left , a steady discontinuity at the interface between the left trace 0.58 and the right trace 0.42 and

the constant state 0.66 connected to the right trace 0.42 on the right. Note that the solution is not undercompressive as $f^{-\prime}(0.58) = f^{+\prime}(0.42) \equiv 0$. We remark that the above fluxes f^- and f^+ do not satisfy the "crossing condition" of [19] and the entropy theory developed in the above reference does not apply to this situation. But we can still compute the solutions given by AV as the scheme is well defined. We present the solutions in figure (6.10). We consider the mesh size $h = 0.1$ and the CFL parameter is $\lambda = 0.125$.

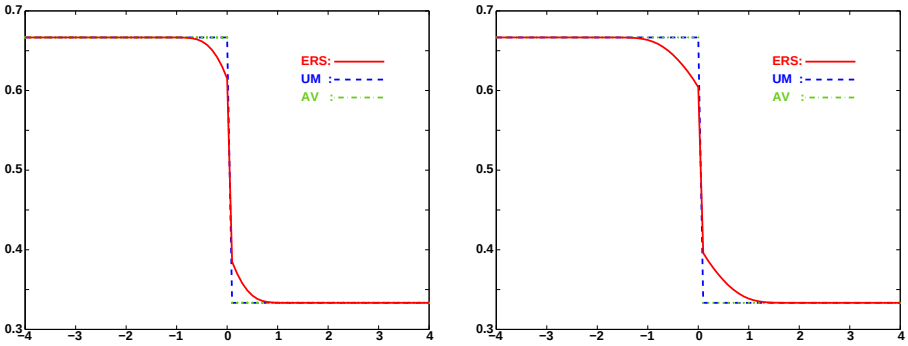

Figure 6.10: Solutions in experiment 4 with h = 0.1 at t=1.5 and t=3

As shown in Fig. 6.10), the solution obtained with ERS approximates the entropy solution of [2]. Note that the left and right traces are very close to the expected values of 0.58 and 0.42. On the other hand, the solution computed by both UM and AV is the steady state 2/3 on the left and 1/3 on the right which is very different from that of the solution given by ERS. Observe that this solution is undercompressive i.e $f^{-\prime}(2/3) < 0$ and $f^{+\prime}(1/3) > 0$. The entropy theory of [2] avoids solutions of this type. Also this solution differs from the solution of the Riemann problem constructed by Diehl in [12] which in this case is identical to the solution computed by ERS. We believe that this undercompressive solution is unphysical and the right solution is computed by ERS.

It is easy to show by using that $\lambda_1^+(2/3) = \lambda_1^-(1/3)$ and $\lambda_2^+(1/3) = \lambda_1^-(2/3)$ and the explicit definition of UM that the solution computed by UM for all h in this case is the steady state with 2/3 on the left and 1/3 on the right. The natural question that arises is whether the solutions computed by UM agree with that of AV in the case where the flux functions intersect in an overcompressive manner. The answer to this question is contained in the next experiment.
Experiment 5 In this experiment, we consider the following flux functions and parameters,

$$\begin{array}{lllllll} \lambda_1^+(S) & = & 50S^2 & \lambda_2^+(S) & = & 5(1-S)^2 \\ \lambda_1^-(S) & = & 10S^2 & \lambda_2^-(S) & = & 20(1-S)^2 \\ g_1 & = & 2 & g_2 & = & 1 \\ \phi & = & 1 & q & = & 0 \end{array}$$

The flux functions are shown in Fig. 6. Notice that in this case, the flux functions intersect in the interior of the domain at 0.46 and the point of intersection is overcompressive.

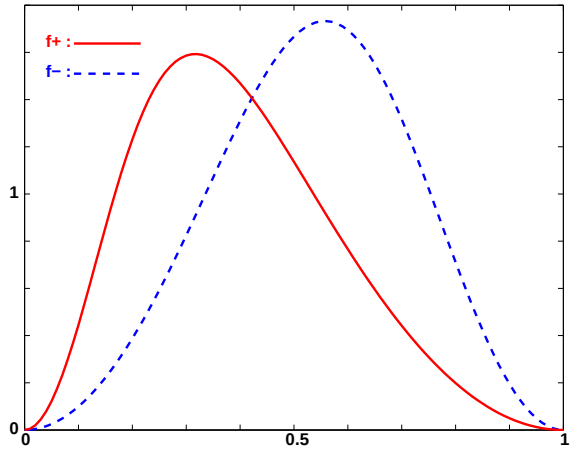

Figure 6.11: Flux functions in experiment 5

We consider the following initial data $S_0(x) = \begin{cases} 0.8 & \text{if} \quad x < 0 \\ 0.2 & \text{if} \quad x > 0. \end{cases}$

In this case, the entropy solution of [2] consists of a rarefaction joining the constant state of 0.8 with the left trace of 0.6, followed by a constant state of 0.6, a steady discontinuity joining the left trace of 0.6 and the right trace 0.32 and a rarefaction joining the right trace to that of the constant state of 0.2. Check that this solution is not undercompressive. The solutions obtained by all the three schemes with $h = 0.1$ and $\lambda = 1/32$ are shown in Fig. 6.12. The solution given by the ERS flux approximates well the entropy solution, even with a large mesh size. The solution given by thg AV flux is quite different in this case and note that the traces $(0.7, 0.22)$ are undercompressive. On the other hand, the solutions obtained by the UM flux are very close to those of the ERS flux besides a boundary layer on the right. A further reduction in mesh size to $h = 0.01$ shows that the boundary layer on the right remains and the traces given by the AV flux are undercompressive as shown in Fig. (6.13).

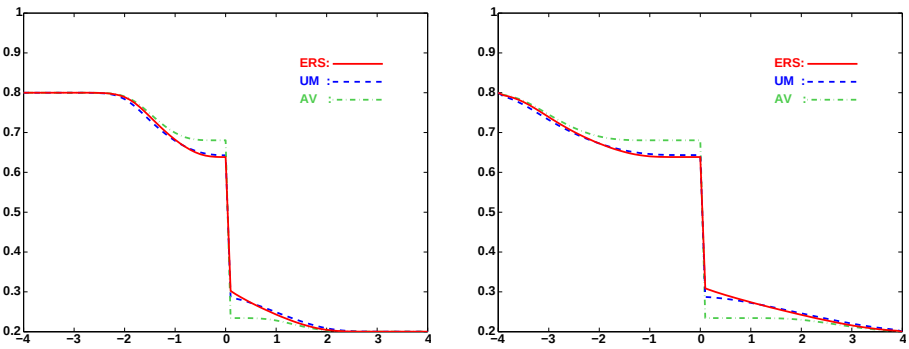

Figure 6.12: Solutions in experiment 5 with h = 0.1 at t=0.25 and t=0.5

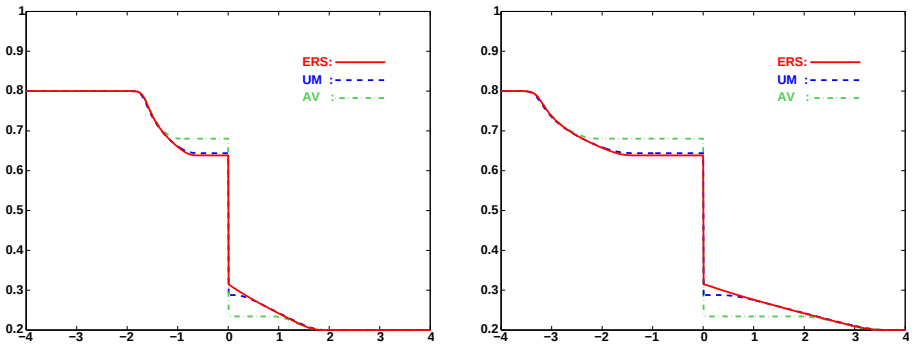

Figure 6.13: Solutions in experiment 5 with h = 0.01 at t=0.25 and t=0.5

To sum up about these experiments we observed the following behaviour across the interface:

1. In some experiments (experiments 1,2,5) the upstream mobility flux may produce unphysical boundary layers and travelling waves. The traveling wave and the width of the boundary layer vanishes when $h \to 0$, while the heigth of the boundary layer may remain significant. Despite of these numerical artefacts the solution given by the upstream mobility flux remain close to that given by the ERS flux. This suggests that in these experiments, the solution calculated with the UM flux, even though it does not satisfy the pointwise entropy condition (3.3), may satisfy some integral form of it. For the average flux, depending on the experiment, it behaves like the UM flux (experiments 1, 5) or it misses the interface discontinuity (experiment 2).

2. In other experiments (experiment 3, 4) the UM flux as well as the AV flux produces unphysical undercompressive solutions (experiment 4) and even misses the interface discontinuity (experiment 3).

7 Conclusion

In this paper we analyzed the upstream mobility numerical flux for a finite difference scheme when a two-phase flow crosses the interface between two rock types. This results in a discontinuity in the flux function with respect to the space variable. We were able to prove convergence to a weak solution but numerical experiments show that it does not satisfy the entropy condition of [2].

Most often the solution given by the upstream mobility flux is close to that given by the extended Godunov flux but numerical artefacts like boundary layers or traveling waves perturb the solution. There are even cases when the upstream mobility flux misses the discontinuity at the interface. The solution given by the averaged flux is not doing any better.

Acknowledgements

The authors would like to thank Professor Adimurthi and Professor G.D.Veerappa Gowda for their useful suggestions and discussions.

References

[1] Adimurthi and G.D.Veerappa Gowda, *Conservation Laws with Discontinuous flux*, Journal of Mathematics, Kyoto university , 43 (2003), pp. 27-70.

[2] Adimurthi,J. Jaffré and G.D.Veerappa Gowda, *Godunov type methods for Scalar Conservation Laws with Flux function discontinuous in the space variable*, SIAM J. Numer. Anal., 42 (2004), pp. 179-208.

[3] Adimurthi, Siddhartha Mishra and G.D.Veerappa Gowda, *Optimal entropy solutions for conservation laws with discontinuous flux functions*, Journal of Hyperbolic Differential Equations, 2 (2005), pp. 783-837.

[4] Adimurthi, Siddhartha Mishra and G.D.Veerappa Gowda, *Godunov type methods for conservation laws with flux functions discontinuous in the space variable -II: Convex-concave type fluxes and generalized entropy solutions*, Journal of Computational and Applied Mathematics, 203 (2007), pp. 310-344.

[5] Adimurthi, Siddhartha Mishra and G.D.Veerappa Gowda, *Existence and stability of entropy solutions for conservation laws with discontinuous non-convex fluxes*, Networks and Heterogeneous Media, 2 (2007), pp. 127-157.

[6] Adimurthi, Siddhartha Mishra and G.D.Veerappa Gowda, *Convergence of Godunov type schemes for a conservation laws with a spatially varying discontinuous flux function*, Math. Comp., 76 (2007), pp. 1219-1242.

[7] K. Aziz and A. Settari,*Petroleum Reservoir Simulation*, Applied Sciense Publishers, London, 1979.

[8] R. Burger,K.H. Karlsen,N.H. Risebro and J.D. Towers,*Well-posedness in BV_t and convergence of a difference scheme for continuous sedimentation in ideal clarifier thickener units*, Numer. Math, 97 (2004), pp. 25-65.

[9] Y. Brenier and J. Jaffré, *Upstream differencing for multiphase flow in resorvoir simulation*, SIAM J. Numer. Anal., 28 (1991), pp. 685-696.

[10] G.M. Coclite and N.H. Risebro, *Conservation Laws with time dependent discontinuous coefficients*, SIAM J. Numer. Anal., 36 (2005), pp. 1293-1309.

[11] M. G. Crandall and A. Majda, Monotone difference approximations for scalar conservation laws., Math. Comp. 34 (1980), pp. 1–2.

[12] S. Diehl, *On scalar conservation laws with point source and discontinuous flux function modeling continuous sedimentation*, SIAM J. Math. Anal., 26(6) (1995), pp. 1425-1451.

[13] S. Diehl, *A conservation law with point source and discontinuous flux function modelling continuous sedimentation*, SIAM J. Appl. Math., 56(2) (1996), pp. 388-419.

[14] T. Gimse and N.H. Risebro, *Riemann problems with discontinuous flux function*, In Proc. 3rd Internat. Conf. Hyperbolic problems Studentlitteratur, Uppsala,1991, pp. 488-502.

[15] T. Gimse and N.H. Risebro, *Solution of Cauchy problem for a conservation law with a discontinuous flux function*, SIAM J. Math. Anal, 23(3), (1992), pp. 635-648.

[16] E. Godlewski and P.A. Raviart, *Hyperbolic systems of Conservation laws*, Mathematiques et Applications,Ellipses, Paris,1991.

[17] S. Godunov, *Finite difference methods for numerical computation of discontinuous solutions of the equations of fluid dynamics*, Math. Sbornik, 47 (1959), pp. 271-306.

[18] K.H. Karlsen,N.H. Risebro and J.D. Towers, *Upwind difference approximations for degenerate parabolic convection-diffusion equations with a discontinuous coefficient*, IMA J. Numer. Anal., 22 (2002), pp. 623-664.

[19] K.H. Karlsen,N.H. Risebro and J.D. Towers, L^1 *stability for entropy solution of nonlinear degenerate parabolic convection-diffusion equations with discontinuous coefficients*, Skr. K. Nor. Vidensk. Selsk.,no 3, (2003), 49 pages.

[20] J. Jaffré, *Numerical calculation of the flux across an interface between two rock types of a porous medium for a two-phase flow.* In Hyperbolic Problems: Theory, Numerics, Applications, J. Glimm, M.J. Graham, J.W. Grove and B.J. Plohr Eds. (World Scientific, Singapore, 1996), pp. 165-177.

[21] E. Kaasschieter, Solving the Buckley-Leverret equation with gravity in a heteregenous porous media, Computational Geosciences, 3 (1999), pp. 23-48.

[22] N. N. Kuznecov and S. A. Volosine, *Monotone difference approximations for a first order quasilinear equation* , Soviet Math. Dokl. 17 (1976), pp. 1203-1206.

[23] S. Mochon, *An analysis for the traffic on highways with changing surface conditions*, Math. Model., 9 (1987), pp. 1-11.

[24] D.A.Ross, *Two new moving boundary problems for scalar conservation laws*, Communications in Pure and Applied Mathematics, 41 (1988), pp. 725-737.

[25] P.H. Sammon, *An analysis of upstream differencing*, SPE Reservoir Engineering, 3 (1988), pp. 1053-1056.

[26] Siddhartha Mishra, *Scalar Conservation Laws with Discontinuous flux*, M.S thesis, Indian Institute of Science, Bangalore,India, 2003.

[27] Siddhartha Mishra, *Convergence of upwind finite difference schemes for a scalar conservation law with indefinite discontinuities in the flux function*, SIAM J. Numer. Anal., 43 (2005), pp. 559-577.

[28] B. Temple,*Global solution of the Cauchy problem for a class of* 2×2 *nonstrictly hyperbolic conservation laws*, Adv. in Appl. Math.,3 (1982), pp. 335-375.

[29] J.D. Towers,*Convergence of a difference scheme for conservation laws with a discontinuous flux*, SIAM J. Numer. Anal., 38 (2000), pp. 681-698.

[30] J.D. Towers,*A difference scheme for conservation laws with a discontinuous flux: The nonconvex case*, SIAM J. Numer. Anal., 39 (2001), pp. 1197-1218.

Centre de recherche INRIA Paris – Rocquencourt
Domaine de Voluceau - Rocquencourt - BP 105 - 78153 Le Chesnay Cedex (France)

Centre de recherche INRIA Bordeaux – Sud Ouest : Domaine Universitaire - 351, cours de la Libération - 33405 Talence Cedex
Centre de recherche INRIA Grenoble – Rhône-Alpes : 655, avenue de l'Europe - 38334 Montbonnot Saint-Ismier
Centre de recherche INRIA Lille – Nord Europe : Parc Scientifique de la Haute Borne - 40, avenue Halley - 59650 Villeneuve d'Ascq
Centre de recherche INRIA Nancy – Grand Est : LORIA, Technopôle de Nancy-Brabois - Campus scientifique
615, rue du Jardin Botanique - BP 101 - 54602 Villers-lès-Nancy Cedex
Centre de recherche INRIA Rennes – Bretagne Atlantique : IRISA, Campus universitaire de Beaulieu - 35042 Rennes Cedex
Centre de recherche INRIA Saclay – Île-de-France : Parc Orsay Université - ZAC des Vignes : 4, rue Jacques Monod - 91893 Orsay Cedex
Centre de recherche INRIA Sophia Antipolis – Méditerranée : 2004, route des Lucioles - BP 93 - 06902 Sophia Antipolis Cedex

Éditeur
INRIA - Domaine de Voluceau - Rocquencourt, BP 105 - 78153 Le Chesnay Cedex (France)
http://www.inria.fr
ISSN 0249-6399